Original Article
ISSN (Online): 2582-7472

ShodhKosh: Journal of Visual and Performing Arts
June 2024 5(6), 2890–2902

SOLITON EXCITATIONS IN AN (3+1) DIMENSIONAL ALPHA-HELIX PROTEIN SYSTEM WITH QUADRAPOLE-QUADRAPOLE INTERACTIONS

R. Jeba Vijitha [1], S. Beauno [2]

[1] Reg.No.21213282132009, Research Scholar, Department of Physics, Women's Christian College, Nagercoil 629001, Tamilnadu, India
[2] Affiliated to Manonmaniam Sundaranar University, Abishekapatti, Tirunelveli 627 012, Tamilnadu, India

Corresponding Author
S. Beauno, beunaphysics@gmail.com

DOI
10.29121/shodhkosh.v5.i6.2024.3464

Funding: This research received no specific grant from any funding agency in the public, commercial, or not-for-profit sectors.

ABSTRACT
This paper aims to explore that the soliton solutions for the three-dimensional (3D) model Hamiltonian equation, specifically as it pertains to protein molecules. The considered equation has been thoroughly analyzed that, with every step of the calculations discussed in detail and the main results are clearly explained. Notably, eight distinct types of the soliton structures are identified and the surfaces corresponding to each solitons solution are graphically illustrated as described. The explicit forms of the eight soliton solutions are presented. Additionally, mathematical derivations and numerical graphs are provided to support and visualize the soliton solutions of the energy equation.

Keywords: Protein, Alpha Helix, Soliton

1. INTRODUCTION
Proteins are large, complex molecules that play critical roles in nearly every biological process. They are essential components of all living organisms and are involved in a vast array of the cellular functions, including structure, function, regulation, and catalysis of biochemical reactions [1][2][3]. Proteins are made up of amino acids, which are organic compounds containing both amino (-NH_2) and carboxyl (-COOH) functional groups. There are 20 different amino acids that combine in various sequences to form proteins [4][5]. The sequence of amino acids in a protein is known as its primary structure. The primary structure is the linear sequence of amino acids in a polypeptide chain [6][7]. The sequence determines how the protein will fold into its unique three-dimensional shape, which is essential for its function [8]. Amino acids are linked by peptide bonds (covalent bonds formed during protein synthesis). The primary structure of insulin consists of two polypeptide chains with specific amino acid sequences [9]. Proteins are enzymes act as

catalysts, speeding up biochemical reactions. Structural proteins, such as collagen in connective tissues and keratin in hair and nails, provide mechanical support and strength [10][11]. Proteins like hemoglobin transports oxygen in the blood, while membrane transporters facilitate the movement of molecules across cell membranes.

Solitons can be defined as wave forms whose configuration remains undisturbed in the course of time of propagation. In other words, they do not dissipate or evolve in different manners as they travel [12][13]. Owing to this unique feature that is inherent in the behavior of solitons, such waves tend to stand out from other wave phenomena supported by linear mediums which tend to spread or decrease in strength. The ‘soliton’ term was first used in the ‘fluid dynamics’ context in the 19th century after John Scott Russell had observed a wave which was moving along a canal without changing its shape. Thereafter the concepts about the solitons were adopted in a number of disciplines including but not limited to physics, mathematics and engineering [14][15]. These solitons are the classic types of slow-moving waveforms, found often in the study of shallow water waves within the KdV soliton solutions. KdV solitons are quite smooth as they take a solitary shape and as such become the prototype for such legislators in shallow waters [16]. Sine-Gordon Solitons are periodic in nature. These solitons are ordinarily periodic and thus can be defined in terms of periodic functions like sine and cosine [17][18][19].

The organization of this paper is as follows: Section 2: We introduce the three-body problem in the context of the Hamiltonian equation derived from the Schrödinger equation. The quadrupole-quadrupole mode of interaction is analyzed and solved by using a Taylor series expansion. This section lays the foundational framework for the mathematical model and its relevance to protein molecules. Section 3: This section focuses on applying the perturbation technique to derive soliton solutions. Also the effect of inhomogeneity in protein molecules is examined in this section. Section 4: The methodology is carefully explained and the propagation of eight distinct soliton structures within protein molecules is explored. Each soliton solution is thoroughly discussed and graphically illustrated to provide a clear understanding of their behavior and characteristics. The impact of inhomogeneities on soliton dynamics is analyzed, offering insights into the complex interactions within the system and their influence on soliton propagation.

2. HAMILTONIAN WITH QUADRUPOLE-QUADRUPOLE INTERACTION

We consider a model representing an inhomogeneous alpha-helix protein chain incorporating quadrupole-quadrupole interactions. In this model, the interplay between neighboring chains of protein molecules is taken into account, which leads to a (3+1)-dimensional representation. This approach extends the dimensionality to include three spatial dimensions and one temporal dimension, providing a more comprehensive framework for analyzing protein dynamics. The model is based on a modified version of the Davydov Hamiltonian [20][21][22][23][24], where the traditional assumptions are adapted to incorporate the effects of inhomogeneity and quadrupole-quadrupole interactions. This modification allows us to capture the complex interactions and energy transfer mechanisms within the alpha-helix structure more accurately. Such considerations are crucial for understanding the dynamic behavior and soliton propagation in protein molecules under realistic biological conditions. The suitable model of modifying Davydov Hamiltonian, where

$$H_{3D} = H_{ph} - H_{ex} - H_{ph-ex} \tag{1}$$

Intra-chain Hamiltonian (H_{ex}): This represents the energy contributions within a single chain. It includes terms that describe the exciton motion and interaction with the lattice vibrations (phonons).

$$H_{\mathrm{ex}} = \sum_{\ell,\iota,J} \{B^{\dagger}_{\ell,\iota,J} E_0 B_{\ell,\iota,J} + B^{\dagger}_{\ell,\iota,J} E_1 B_{\ell,\iota,J} B^{\dagger}_{\ell,\iota,J} B_{\ell,\iota,J} - J_0 F_{\ell,\iota,J} (B^{\dagger}_{\ell,\iota,J} B_{\ell+1,\iota,J} +$$

$$B_{\ell,\iota,J} B^{\dagger}_{\ell+1,\iota,J}) - J_0' F_{\ell,\iota,J} (B^{\dagger}_{\ell,\iota,J} B_{\ell,\iota+1,J} + B_{\ell,\iota,J} B^{\dagger}_{\ell,\iota+1,J}) - J_0'' F_{\ell,\iota,J} (B^{\dagger}_{\ell,\iota,J}$$

$$B_{\ell,\iota,J+1} + B_{\ell,\iota,J} B^{\dagger}_{\ell,\iota,J+1}) - J_1 F_{\ell,\iota,J} (B^{\dagger}_{\ell,\iota,J} B_{\ell+1,\iota+1,J+1} + B_{\ell,\iota,J}$$

$$B^{\dagger}_{\ell+1,\iota+1,J+1}) - J_1' F_{\ell,\iota,J} (B^{\dagger}_{\ell,\iota,J} B_{\ell+1,\iota+1,J-1} + B_{\ell,\iota,J} B^{\dagger}_{\ell+1,\iota+1,J-1})$$

$$-J_1'' F_{\ell,\iota,J} (B^{\dagger}_{\ell,\iota,J} B_{\ell+1,\iota-1,J-1} + B_{\ell,\iota,J} B^{\dagger}_{\ell+1,\iota-1,J-1}) - J_2 F_{\ell,\iota,J} (B^{\dagger}_{\ell,\iota,J}$$

$$B_{\ell+1,\iota+1,J} + B_{\ell,\iota,J} B^{\dagger}_{\ell+1,\iota+1,J}) - J_2' F_{\ell,\iota,J} (B^{\dagger}_{\ell,\iota,J} B_{\ell+1,\iota,J+1} + B_{\ell,\iota,J}$$

$$B^{\dagger}_{\ell+1,\iota,J+1}) - J_2'' F_{\ell,\iota,J}\big(B^{\dagger}_{\ell,\iota,J} B_{\ell,\iota+1,J+1} + B_{\ell,\iota,J} B^{\dagger}_{\ell,\iota+1,J+1}\big)\} \quad (2)$$

Phonon Hamiltonian (H_{ph}): This term describes the energy of lattice vibrations:

$$H_{\text{ph}} = \sum_{\ell,\iota,J} \{\frac{P^2{}^{\wedge}_{\ell,\iota,J}}{2M} + \frac{K}{2}[(U_{\ell,\iota,J} - U_{\ell-1,\iota,J})^2 + (U_{\ell,\iota,J} - U_{\ell,\iota-1,J})^2 + (U_{\ell,\iota,J} - U_{\ell,\iota,J-1})^2]\} \quad (3)$$

The exciton and phonon interaction

$$H_{\text{ph-ex}} = \sum_{\ell,\iota,J} \{\chi_1 B^{\dagger}_{\ell,\iota,J} B_{\ell,\iota,J}[U_{\ell+1,\iota,J} - U_{\ell-1,\iota,J} + U_{\ell,\iota+1,J} - U_{\ell,\iota-1,J} + U_{\ell,\iota,J+1} - U_{\ell,\iota,J-1}] + \chi_2 B^{\dagger}_{\ell,\iota,J} B_{\ell,\iota,J}[U_{\ell+1,\iota,J} - U_{\ell-1,\iota,J} + U_{\ell,\iota+1,J} - U_{\ell,\iota-1,J} + U_{\ell,\iota,J+1} - U_{\ell,\iota,J-1}]\} \quad (4)$$

Using Davydov model, the collective excitation of coherent state is written as

$$H_{3D} = \sum_{\ell,\iota,J} \{\phi^{\dagger}_{\ell,\iota,J} E_0 \phi_{\ell,\iota,J} + \phi^{\dagger}_{\ell,\iota,J} E_1 \phi_{\ell,\iota,J} \phi^{\dagger}_{\ell,\iota,J} \phi_{\ell,\iota,J} - J_0 F_{\ell,\iota,J}(\phi^{\dagger}_{\ell,\iota,J} \phi_{\ell+1,\iota,J} + \phi_{\ell,\iota,J} \phi^{\dagger}_{\ell+1,\iota,J}) - J_0' F_{\ell,\iota,J}(\phi^{\dagger}_{\ell,\iota,J} \phi_{\ell,\iota+1,J} + \phi_{\ell,\iota,J} \phi^{\dagger}_{\ell,\iota+1,J}) - J_0'' F_{\ell,\iota,J}(\phi^{\dagger}_{\ell,\iota,J} \phi_{\ell,\iota,J+1} + \phi_{\ell,\iota,J} \phi^{\dagger}_{\ell,\iota,J+1}) - J_1 F_{\ell,\iota,J}(\phi^{\dagger}_{\ell,\iota,J} \phi_{\ell+1,\iota+1,J+1} + \phi_{\ell,\iota,J} \phi^{\dagger}_{\ell+1,\iota+1,J+1}) - J_1' F_{\ell,\iota,J}(\phi^{\dagger}_{\ell,\iota,J} \phi_{\ell+1,\iota+1,J-1} + \phi_{\ell,\iota,J} \phi^{\dagger}_{\ell+1,\iota+1,J-1}) - J_1'' F_{\ell,\iota,J}(\phi^{\dagger}_{\ell,\iota,J} \phi_{\ell+1,\iota-1,J-1} + \phi_{\ell,\iota,J} \phi^{\dagger}_{\ell+1,\iota-1,J-1}) - J_2 F_{\ell,\iota,J}(\phi^{\dagger}_{\ell,\iota,J} \phi_{\ell+1,\iota+1,J} + \phi_{\ell,\iota,J} \phi^{\dagger}_{\ell+1,\iota+1,J}) - J_2' F_{\ell,\iota,J}(\phi^{\dagger}_{\ell,\iota,J} \phi_{\ell+1,\iota,J+1} + \phi_{\ell,\iota,J} \phi^{\dagger}_{\ell+1,\iota,J+1}) - J_2'' F_{\ell,\iota,J}(\phi^{\dagger}_{\ell,\iota,J} \phi_{\ell,\iota+1,J+1} + \phi_{\ell,\iota,J} \phi^{\dagger}_{\ell,\iota+1,J+1}) + \frac{P^2{}^{\wedge}_{\ell,\iota,J}}{2M} + \frac{K}{2}[(U_{\ell,\iota,J} - U_{\ell-1,\iota,J})^2 + (U_{\ell,\iota,J} - U_{\ell,\iota-1,J})^2 + (U_{\ell,\iota,J} - U_{\ell,\iota,J-1})^2] + \chi_1 \phi^{\dagger}_{\ell,\iota,J} \phi_{\ell,\iota,J}[U_{\ell+1,\iota,J} - U_{\ell-1,\iota,J} + U_{\ell,\iota+1,J} - U_{\ell,\iota-1,J} + U_{\ell,\iota,J+1} - U_{\ell,\iota,J-1}] + \phi^{\dagger}_{\ell,\iota,J} \phi_{\ell,\iota,J} \chi_2 \phi^{\dagger}_{\ell,\iota,J} \phi_{\ell,\iota,J}[U_{\ell+1,\iota,J} - U_{\ell-1,\iota,J} + U_{\ell,\iota+1,J} - U_{\ell,\iota-1,J} + U_{\ell,\iota,J+1} - U_{\ell,\iota,J-1}]\} \quad (5)$$

On-site, the excitation energy and the quadrupole excitation of the molecules in a unit cell are denoted as E_0 and E_1. The characteristics $J_0, J_0', J_0'', J_1, J_1', J_1'', J_2, J_2'$ and J_2'' are attached to the quadrupole-quadrupole coupling in the X, Y and Z directions, respectively. Further, χ_1 and χ_2 respectively provide the quadrupole-quadrupole coupling constants, which also indicates the degree of these interactions among the adjacent molecules. Here, $P_{\ell,\iota,J}$ means the conjugate momentum, while M is the molecule's mass. The homogenous hydrogen bonding spine coefficient is $F_{\ell,\iota,J}$. The dynamics of the equation $\phi_{\ell,\iota,J}$, $U_{\ell,\iota,J}$ and $P_{\ell,\iota,J}$ can be written as

$$i\hbar \frac{d\Phi_{\ell,\iota,J}}{dt} = E_0 \phi_{\ell,\iota,J} + 2 E_1 \Phi^2_{\ell,\iota,J} \Phi^*_{\ell,\iota,J} - J_0(F_{\ell,\iota,J} \phi_{\ell+1,\iota,J} + F_{\ell-1,\iota,J} \phi_{\ell-1,\iota,J}) - J_0'(F_{\ell,\iota,J} \phi_{\ell,\iota+1,J} + F_{\ell,\iota-1,J} \phi_{\ell,\iota-1,J}) - J_0''(F_{\ell,\iota,J} \phi_{\ell,\iota,J+1} + F_{\ell,\iota,J-1} \phi_{\ell,\iota,J-1}) - J_1(F_{\ell,\iota,J} \phi_{\ell+1,\iota+1,J+1} + F_{\ell-1,\iota-1,J-1} \phi_{\ell-1,\iota-1,J-1}) - J_1'(F_{\ell,\iota,J} \phi_{\ell+1,\iota+1,J-1} + F_{\ell-1,\iota-1,J+1} \phi_{\ell-1,\iota-1,J+1}) - J_1''(F_{\ell,\iota,J} \phi_{\ell+1,\iota-1,J-1} + F_{\ell-1,\iota+1,J+1} \phi_{\ell-1,\iota+1,J+1}) - J_2(F_{\ell,\iota,J} \phi_{\ell+1,\iota+1,J} + F_{\ell-1,\iota-1,J} \phi_{\ell-1,\iota-1,J}) - J_2'(F_{\ell,\iota,J} \phi_{\ell+1,\iota,J-1} + F_{\ell-1,\iota,J+1} \phi_{\ell-1,\iota,J+1}) - J_2''(F_{\ell,\iota,J} \phi_{\ell,\iota-1,J-1} + F_{\ell,\iota+1,J+1} \phi_{\ell,\iota+1,J+1}) + \chi_1 \phi_{\ell,\iota,J} (U_{\ell+1,\iota,J} - U_{\ell-1,\iota,J}$$

$$+U_{\ell,\iota+1,J}-U_{\ell,\iota-1,J}+U_{\ell,\iota,J+1}-U_{\ell,\iota,J-1})+2\chi_2\Phi^2_{\ell,\iota,J}\Phi^*_{\ell,\iota,J}(U_{\ell+1,\iota,J}$$
$$-U_{\ell-1,\iota,J}+U_{\ell,\iota+1,J}-U_{\ell,\iota-1,J}+U_{\ell,\iota,J+1}-U_{\ell,\iota,J-1}) \quad (6)$$

$$M\frac{d^2U_{\ell,\iota,J}}{dt^2}=-\mathrm{k}\,(6U_{\ell,\iota,J}-U_{\ell+1,\iota,J}-U_{\ell-1,\iota,J}-U_{\ell,\iota+1,J}-U_{\ell,\iota-1,J}-U_{\ell,\iota,J+1}-U_{\ell,\iota,J-1})+$$
$$\chi_1(|\phi_{\ell+1,\iota,J}|^2-|\phi_{\ell-1,\iota,J}|^2+|\phi_{\ell,\iota+1,J}|^2-|\phi_{\ell,\iota-1,J}|^2+|\phi_{\ell,\iota,J+1}|^2-|\phi_{\ell,\iota,J-1}|^2)$$
$$\chi_2(|\phi_{\ell+1,\iota,J}|^4-|\phi_{\ell-1,\iota,J}|^4+|\phi_{\ell,\iota+1,J}|^4-|\phi_{\ell,\iota-1,J}|^4+|\phi_{\ell,\iota,J+1}|^4-|\phi_{\ell,\iota,J-1}|^4) \quad (7)$$

In the study of the higher-dimensional alpha-helical proteins, moving from a discrete to a continuum representation simplifies the analysis by replacing discrete variables with continuous fields. The dynamics represented by Eqns. (6) and (7) in discrete form involves the lattice points describing variables like exciton amplitudes and phonon displacements at the discrete sites along the protein chains. Transition in to the continuum limit, we express the discrete variables in terms of continuous variables and expand them around their positions using a Taylor series. The coupled equation describes the interaction of excitons (energy carriers) and phonons (vibrations), crucial for understanding the energy transport and the stability in alpha-helical proteins. We get

$$M\,U_{ttt}=-k\ \in^2\ (U_{xx}+U_{yy}+U_{zz})+2\,(\chi_1+\chi_2)(|\Phi|^2{}_x+|\Phi|^2{}_y+|\Phi|^2{}_z)]\in \quad (8)$$

$$i\,\phi=-C_1\,\phi-C_2\phi_x-C_3\phi_y-C_4\phi_z-C_5\phi_{xx}-C_6\phi_{yy}-C_7\phi_{zz}-C_8\phi_{xy}-C_9\phi_{yz}-$$
$$C_{10}\phi_{xz}+C_{11}|\phi|^2\,\phi+C_{12}|\phi|^4\,\phi=0 \quad (9)$$

The wave variables, $\xi=\ K_1\,x+K_2\,y+K_3\,z$ in Eqns. (8, 9), to obtain

$$i\,\phi_t+C_1\,\phi+C_2\phi_x+C_3\phi_y+C_4\phi_z+C_5\phi_{xx}+C_6\phi_{yy}+C_7\phi_{zz}+C_8\phi_{xy}+C_9\phi_{yz}+C_{10}\phi_{xz}-C_{11}|\phi|^2\,\phi-C_{12}|\phi|^4\,\phi=0 \quad (10)$$

Where $C_1=\frac{-6\,F\,\Phi[J_0'+J_1'+J_2'-E_0]}{\hbar}+\frac{\in F_X\,[J_0'+3\,J_1'+2\,J_2']\Phi}{\hbar}+\frac{\in F_Y\,[J_0'+J_1'+2\,J_2']\Phi}{\hbar}+\frac{\in F_Z\,[J_0'-J_1'+2\,J_2']\Phi}{\hbar}-\frac{\in^2}{2}\frac{F_{XX}[J_0'+3\,J_1']\Phi}{\hbar}-\frac{\in^2}{2}\frac{F_{YY}[J_0'+3\,J_1']\Phi}{\hbar}-\frac{\in^2}{2}\frac{F_{ZZ}[J_0'+3\,J_1']\Phi}{\hbar}-\frac{\in^2(F_{XX}+F_{YY}+F_{ZZ})J_2'\Phi}{\hbar}-\frac{\in^2F_{XY}[J_1'+J_2']\Phi}{\hbar}-\frac{\in^2F_{YZ}[J_1'+J_2']\Phi}{\hbar}+\frac{\in^2F_{ZX}[J_1'-J_2']\Phi}{\hbar}$, $C_2=[\frac{-\in^2F_X\,[J_0'+3\,J_1'+2\,J_2']}{\hbar}-\frac{\in^2F_Y[\,J_1'+J_2']}{\hbar}+\frac{\in^2F_Z[\,J_1'-J_2']}{\hbar}+\frac{\in^3}{2}\frac{F_{XX}[J_0'+3\,J_1'+J_2']}{\hbar}+\frac{\in^3}{2}\frac{F_{YY}[3\,J_1'+J_2']}{\hbar}+\frac{\in^3}{2}\frac{F_{ZZ}[3\,J_1'+J_2']}{\hbar}+\frac{\in^3F_{XY}[\,J_1'+J_2']}{\hbar}-\frac{\in^3F_{YZ}J_1'}{\hbar}-\frac{\in^3F_{ZX}[\,J_1'-J_2']}{\hbar}]\Phi_X$,
$C_3=[\frac{-\in^2F_X\,[J_1'+J_2']}{\hbar}-\frac{\in^2F_Y[J_0'+3\,J_1'+2\,J_2']}{\hbar}-\frac{\in^2F_Z[\,J_1'+J_2']}{\hbar}+\frac{\in^3}{2}\frac{F_{XX}[J_1'+J_2']}{\hbar}+\frac{\in^3}{2}\frac{F_{YY}[J_0'+J_1'+2\,J_2']}{\hbar}+\frac{\in^3}{2}\frac{F_{ZZ}[\,J_1'+J_2']}{\hbar}+\frac{\in^3F_{XY}[\,J_1'+J_2']}{\hbar}+\frac{\in^3F_{YZ}[J_1'+J_2']}{\hbar}-\frac{\in^3F_{ZX}J_1'}{\hbar}]\Phi_Y$, $C_4=[\frac{\in^2F_X\,[J_1'-J_2']}{\hbar}-\frac{\in^2F_Y[J_1'+J_2']}{\hbar}-\frac{\in^2F_Z[\,J_0'+3\,J_1'+2\,J_2']}{\hbar}-\frac{\in^3}{2}\frac{F_{XX}[J_1'-J_2']}{\hbar}-\frac{\in^3}{2}\frac{F_{YY}[J_1'-J_2']}{\hbar}+\frac{\in^3}{2}\frac{F_{ZZ}[\,J_0'-J_1'+2\,J_2']}{\hbar}-\frac{\in^3F_{XY}J_1'}{\hbar}+\frac{\in^3F_{YZ}[J_1'+J_2']}{\hbar}+\frac{\in^3F_{ZX}[3\,J_1'+J_2']}{\hbar}]\Phi_Z$, $C_5=[\frac{-\in^2F\,[J_0'+3\,J_1'+2\,J_2']}{\hbar}+\frac{\in^2}{2}\frac{F_X[J_0'+3\,J_1'+2\,J_2']}{\hbar}+\frac{\in^3}{2}\frac{F_Y[\,J_1'+J_2']}{\hbar}-\frac{\in^3}{2}\frac{F_Z[\,J_1'-J_2']}{\hbar}-\frac{\in^4}{4}\frac{F_{XX}[J_0'+3\,J_1'+J_2']}{\hbar}-\frac{\in^4}{4}\frac{F_{YY}[\,J_1'+J_2']}{\hbar}-\frac{\in^4}{4}\frac{F_{ZZ}[3\,J_1'+J_2']}{\hbar}-\frac{\in^4}{2}\frac{F_{XY}[\,J_1'+J_2']}{\hbar}-\frac{\in^4}{2}\frac{F_{YZ}J_1'}{\hbar}-\frac{\in^4}{2}\frac{F_{ZX}[\,J_1'+J_2']}{\hbar}]\Phi_{XX}$, $C_6=[\frac{-\in^2F\,[J_0'+3\,J_1'+2\,J_2']}{\hbar}+\frac{\in^3}{2}\frac{F_X[\,3\,J_1'+J_2']}{\hbar}+\frac{\in^3}{2}\frac{F_Y[\,J_0'+J_1'+2\,J_2']}{\hbar}-\frac{\in^3}{2}\frac{F_Z[\,J_1'-J_2']}{\hbar}-\frac{\in^4}{4}\frac{F_{XX}[3\,J_1'+J_2']}{\hbar}-\frac{\in^4}{4}\frac{F_{YY}[J_0'+J_1'+J_2']}{\hbar}-\frac{\in^4}{4}\frac{F_{ZZ}[3\,J_1'+J_2']}{\hbar}-\frac{\in^4}{2}\frac{F_{XY}[\,J_1'+J_2']}{\hbar}-\frac{\in^4}{2}\frac{F_{YZ}\,[\,J_1'+J_2']}{\hbar}-\frac{\in^4}{2}\frac{F_{ZX}J_1'}{\hbar}]\Phi_{YY}$, $C_7=[\frac{-\in^2F\,[J_0'+3\,J_1'+2\,J_2']}{\hbar}+\frac{\in^3}{2}\frac{F_X[\,3\,J_1'+J_2']}{\hbar}+\frac{\in^3}{2}\frac{F_Y[\,J_1'+J_2']}{\hbar}-\frac{\in^3}{2}\frac{F_Z[J_0'-J_1'+2\,J_2']}{\hbar}-\frac{\in^4}{4}\frac{F_{XX}[3\,J_1'+J_2']}{\hbar}-\frac{\in^4}{4}\frac{F_{YY}[\,J_1'+J_2']}{\hbar}-\frac{\in^4}{4}\frac{F_{ZZ}[J_0'+3\,J_1'+J_2']}{\hbar}-\frac{\in^4}{2}\frac{F_{XY}J_1'}{\hbar}-\frac{\in^4}{2}\frac{F_{YZ}\,[\,J_1'+J_2']}{\hbar}-\frac{\in^4}{2}\frac{F_{ZX}[\,J_1'+J_2']}{\hbar}]\Phi_{ZZ}$, $C_8=[\frac{-\in^2F\,[\,J_1'+J_2']}{\hbar}+\in^3\,\frac{F_X[\,J_1'+J_2']}{\hbar}+\in^3\,\frac{F_Y[3\,J_1'+J_2']}{\hbar}+\in^3\,\frac{F_ZJ_1'}{\hbar}-\frac{\in^4}{2}\frac{F_{XX}[\,J_1'+J_2']}{\hbar}-\frac{\in^4}{2}\frac{F_{YY}[\,J_1'+J_2']}{\hbar}-\frac{\in^4}{2}\frac{F_{ZZ}J_1'}{\hbar}-\in^4\,\frac{F_{XY}[3\,J_1'+J_2']}{\hbar}-\in^4\,\frac{F_{YZ}\ J_1'}{\hbar}-\in^4\,\frac{F_{ZX}\,J_1'}{\hbar}]\Phi_{XY}$, $C_9=[\frac{-\in^2F\,[\,J_1'+J_2']}{\hbar}+\in^3\,\frac{F_XJ_1'}{\hbar}-\in^3\,\frac{F_Y[\,J_1'-J_2']}{\hbar}+\in^3\,\frac{F_Z[\,J_1'+J_2']}{\hbar}-\frac{\in^4}{2}\frac{F_{XX}J_1'}{\hbar}-\frac{\in^4}{2}\frac{F_{YY}[\,J_1'+J_2']}{\hbar}-\frac{\in^4}{2}\frac{F_{ZZ}[\,J_1'+J_2']}{\hbar}+\in^4\,\frac{F_{XY}J_1'}{\hbar}-\in^4\,\frac{F_{YZ}[3\,J_1'+J_2']}{\hbar}-$

$\in^4 \frac{F_{ZX} J_1'}{\hbar}]\Phi_{YZ}$, $C_{10} = [\frac{-\in^2 F\,[J_1' + J_2']}{\hbar} - \in^3 \frac{F_X[J_1' - J_2']}{\hbar} - \in^3 \frac{F_Y J_1'}{\hbar} + \in^3 \frac{F_Z[3\,J_1' + J_2']}{\hbar} + \frac{\in^4}{2}\frac{F_{XX}\,[J_1' - J_2']}{\hbar} + \frac{\in^4}{2}\frac{F_{YY} J_1'}{\hbar} + \frac{\in^4}{2}\frac{F_{ZZ}[J_1' - J_2']}{\hbar} + \in^4 \frac{F_{XY} J_1'}{\hbar} - \in^4 \frac{F_{YZ} J_1'}{\hbar} - \in^4 \frac{F_{ZX}[3\,J_1' + J_2']}{\hbar}]\Phi_{ZX}$, $C_{11} = \frac{4 \in \chi_1(\chi_1 + \chi_2)A + 2\,E_1}{\hbar}$ and $C_{12} = \frac{8 \in \chi_2(\chi_1 + \chi_2)A}{\hbar}$.

3. EFFECT OF INHOMOGENEITY

To study the effect of inhomogeneity on the soliton excitations, the sine-cosine function method is a powerful perturbation technique. It leverages the structure of nonlinear wave equations to derive analytical solutions in the form of periodic or localized wave profiles.

3.1 Equation and substitution

Assume that the governing equation for the soliton excitation is given by Eq. (10). The wave function is expressed as:

$u(x, y, z, t) = \Lambda_1 \cos^{\beta 1}(\mu\,\xi), v(x, y, z, t) = \Lambda_2 \cos^{\beta 2}(\mu\,\xi),$

3.2 Separation of Real and Imaginary Parts

Let Eq. (10) be written as in wave variable form:

$$-v_t - C_1 u + C_2 u_x + C_3 u_y + C_4 u_z + C_5 u_{xx} + C_6 u_{yy} + C_7 u_{zz} + C_8 u_{xy} + C_9 u_{yz} + C_{10} u_{zx}$$

$$-C_{11}[u^3 + uv^2] - C_{12}(u^5 + 2u^3v^2 + uv^4) = 0 \qquad (11)$$

$$u_t - C_1 v + C_2 v_x + C_3 v_y + C_4 v_z + C_5 v_{xx} + C_6 v_{yy} + C_7 v_{zz} + C_8 v_{xy} + C_9 v_{yz} + C_{10} v_{zx}$$

$$-C_{11}[u^3 + uv^2] - C_{12}(u^5 + 2u^3v^2 + uv^4) = 0 \qquad (12)$$

Substituting $\Phi = u + iv$, we separate the equation into its real and imaginary parts:

1. Real part:

$$-cv_\xi - C_1 u + C_2 u_\xi + C_3 u_\xi + C_4 u_\xi + C_5 u_{\xi\xi} + C_6 u_{\xi\xi} + C_7 u_{\xi\xi} + C_8 u_{\xi\xi} + C_9 u_{\xi\xi} + C_{10} u_{\xi\xi}$$

$$-C_{11}[u^3 + uv^2] - C_{12}(u^5 + 2u^3v^2 + uv^4) = 0 \qquad (13)$$

2. Imaginary part

$$u_\xi - C_\xi v + C_2 v_\xi + C_3 v_\xi + C_4 v_\xi + C_5 v_{\xi\xi} + C_6 v_{\xi\xi} + C_7 v_{\xi\xi} + C_8 v_{\xi\xi} + C_9 v_{\xi\xi} + C_{10} v_{\xi\xi}$$

$$-C_{11}[u^3 + uv^2] - C_{12}(u^5 + 2u^3v^2 + uv^4) = 0 \qquad (14)$$

3.3 Applying the Sine-Cosine Function Method

To solve these equations, we use the sine-cosine function method, which assumes the solution can be written in terms of periodic trigonometric functions. We obtain

$$\cos^{-1}(\mu\xi) = C_1\Lambda_1 - C_5\Lambda_1\mu^2 - C_6\Lambda_1\mu^2 - C_7\Lambda_1\mu^2 - C_8\Lambda_1\mu^2 - C_9\Lambda_1\mu^2 - C_{10}\Lambda_1\mu^2 \qquad (15)$$

$$\cos^{-2}(\mu\xi)\sin(\mu\xi) = C_2\Lambda_1\mu + C_3\Lambda_1\mu + C_4\Lambda_1\mu \qquad (16)$$

$$\cos^{-3}(\mu\xi) = 2\,C_5\Lambda_1\mu^2 + 2\,C_6\Lambda_1\mu^2 + 2\,C_7\Lambda_1\mu^2 + 2\,C_8\Lambda_1\mu^2 + 2\,C_9\Lambda_1\mu^2 + 2\,C_{10}\Lambda_1\mu^2 - C_{11}\Lambda_1^3 - C_{11}\Lambda_1\Lambda_2^2 \quad (17)$$

$$\cos^{-5}(\mu\xi) = -C_{12}\Lambda_1^5 - 2\,C_{12}\Lambda_1^3\Lambda_1^2 - C_{11}\Lambda_1\Lambda_2^4 \quad (18)$$

$$\cos^{-1}(\mu\xi) = C_1\Lambda_2 - C_5\Lambda_2\mu^2 - C_6\Lambda_2\mu^2 - C_7\Lambda_2\mu^2 - C_8\Lambda_2\mu^2 - C_9\Lambda_2\mu^2 - C_{10}\Lambda_2\mu^2$$

$$\cos^{-2}(\mu\xi)\sin(\mu\xi) = C_2\Lambda_2\mu + C_3\Lambda_2\mu + C_4\Lambda_2\mu \quad (19)$$

$$\cos^{-3}(\mu\xi) = 2\,C_5\Lambda_2\mu^2 + 2\,C_6\Lambda_2\mu^2 + 2\,C_7\Lambda_2\mu^2 + 2\,C_8\Lambda_2\mu^2 + 2\,C_9\Lambda_2\mu^2 + 2\,C_{10}\Lambda_2\mu^2 - C_{11}\Lambda_2^3 - C_{11}\Lambda_2\Lambda_1^2 \quad (20)$$

$$\cos^{-5}(\mu\xi) = -C_{12}\Lambda_2^5 - 2\,C_{12}\Lambda_2^3\Lambda_1^2 - C_{11}\Lambda_2\Lambda_1^4 \quad (21)$$

Here, Λ_1 and Λ_2 are constant parameters. To derive the solution, we balance the linear lower-order derivative terms with the nonlinear terms. This balance condition leads to the following relation:

$$\Lambda = \sqrt{\frac{C_1 - 2\,C_{11}}{4\,C_{12}}}$$

$$\mu = \frac{1}{C_2 + C_3 + C_4 + C_5 + C_6 + C_7 + C_8 + C_9 + C_{10}}$$

Hence the solution becomes

$$u(x,y,z,t) = \Lambda_1 \sec\left[\mu(x+y+z-ct)\right]$$

$$v(x,y,z,t) = \Lambda_2 \sec\left[\mu(x+y+z-ct)\right]$$

4. SOLITON PROPAGATIONS:

4.1. Kick Soliton:

A kick soliton refers to a specialized soliton – a stable wave packet that travels through a nonlinear medium without changing the shape. A kick soliton is considered a soliton solution that possesses a finite speed after an initial “kick” or disturbance [25]. This is attached to the core meaning where solitons are subjected to disturbing forces or modulations. They achieve a non-zero velocity after perturbed or kicked. The shape of the soliton remains almost constant even after motion begins. Sometimes, the speed of a kick soliton and its characteristics is correlated with the energy or the amplitude of the first ‘kick’ delivered to it. Kick solitons are enigmatic but satisfying results of nonlinear wave motion [26][27]. Properties such as the ability to travel with a constant speed while keeping the shape and the dependence of those properties on the initial condition make it an important tool in the study and applications of solitons found in nature and technology.

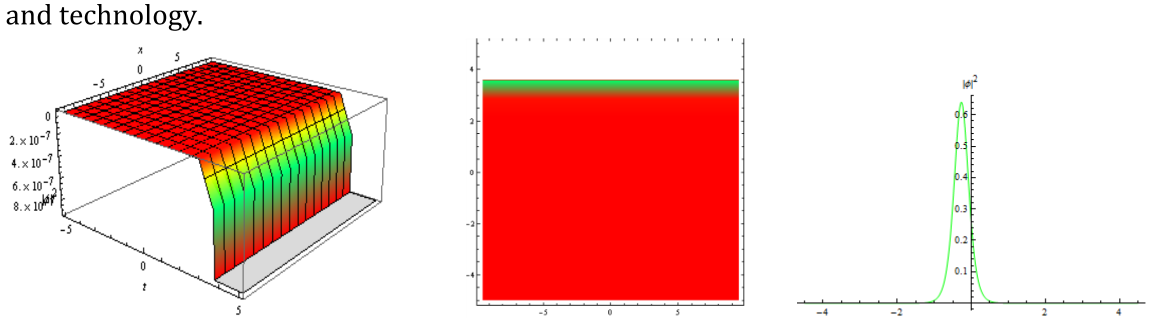

(b) (c)

Figure 1: Behaviour of the kick soliton collision

Fig. (1a), The wave profile translates as a self-contained, stationary curve that travels along the horizontal axis with time. The maximum height of the soliton as well as its entire spread does not change, which emphasizes its reintegrating self-character. Solitons, in contrast to ordinary waves do not spread even as they move. This uniqueness has made them highly useful in many disciplines. In Fig. (1b), a horizontal line is observed at the same level for the entire length of the x-axis. Thus, every point within the limits is probable to happen to the same extent. All the red shade of the graph adds to the uniformity since no area is less or more dense for the plot. The x-axis shows that the variable that is measured and then the y-axis shows the measured variable's density. Fig. (1c), appears to take the shape of a bell, which is indicative of a normal or Gaussian distribution. The crown or apex of the graph is drawn at x = 0 illustrating that the maximum value of the function is at that particular position. The graph in consideration is vertically balanced and symmetrical with respect to the y-axis, which implies that the function take place the same values for x and –x having the same modules. The curve reduces relatively quickly from the 0, x position implies that the function approximates to zero as 'x' approaches either of the infinities.

4.2. Anti-Kick Soliton:

Anti-kick solitons are a specific case of the soliton propagation preservation in a nonlinear medium, which is opposite to the so-called kick solitons. Kick solitons are successfully pushed forward with an effective initial velocity by means of some external disturbance while an anti-kick soliton can be relevant to the situations when the soliton is hindered from moving, stopped or even destroyed by certain factors or forces instead [28][29]. Anti-kick solitons are often associated with dissipative systems where energy is extracted from the soliton. The soliton may become stationary or move very slowly. Specific configurations or external fields counteract the motion of the soliton.

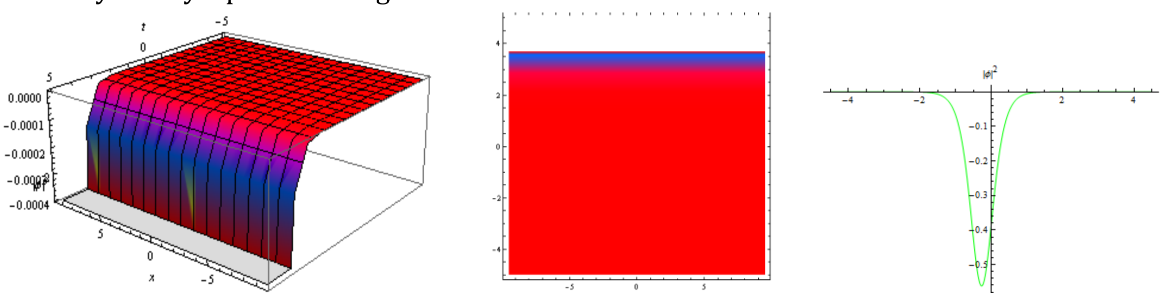

(b) (c)

Figure 2: Anti-kick soliton interaction in protein system

Fig. (2a), the plot most probably is time (t) versus space (x) graph showing how the soliton evolves with time. This type of soliton is a wave confined in space with a stable underlying profile. It propagates towards the positive x-direction while retaining its form, as its characteristic of all the solitons. Fig. (2b), this density plot demonstrates a uniform distribution. The graph exhibits an even height throughout the width of the range, which indicates that the probability of the occurrence of each value within the range is the same. Here, it seems to run from about -8 to 8. The y-axis shows density that is the probability of occurrence of the given value. As it is a uniform distribution all the values in the spread having the same density. Fig. (2c), the graph possesses y-axis symmetry, suggesting that the likelihood of locating the particle at any region to one side of the origin is also the same towards the opposite end of the origin. The highest prominence at the centre or x=0 position denotes where the particle is most likely to be. The amplitude diminishes with the distance from the centre which implies that finding the particle becomes less likely as one move away from the centre. The intercepts of the graph with in the x-axis are primarily referred to as N.B. These are points at which the chances of locating the particle are non-existent. The depiction could also serve as an illustration of a particle confined in a potential well, with the particle's position being most favourable close to the centre.

4.3. Ring Soliton:

The distinctive ring-like structure with a central depression is characteristic of ring solitons. Solitons are solitary wave that maintain their shape and the velocity as they propagate, even after interacting with other solitons [30][31]. The stable and localized nature of the structure is a hallmark of solitons. Ring solitons appear in various physical systems, such as nonlinear-optics, Bose-Einstein condensates and fluid dynamics. They can be used to transmit information or create stable patterns in these systems.

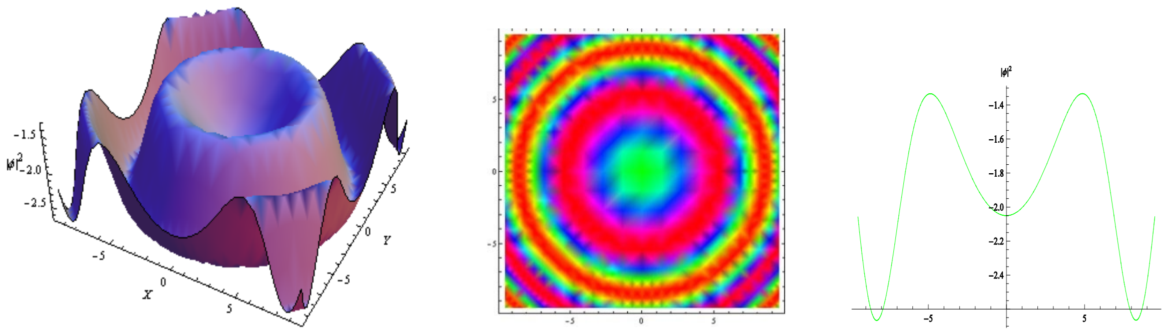

(b) (c)

Figure 3: Bright soliton collision in proteins

From Fig. (3a), solitons arise from balance between the nonlinear and dispersive effects in a medium. Nonlinearity tends to focus the wave, while dispersion tends to spread it out. The central dispersion indicates as a phase singularity, meaning that the waves phase changes by a multiple of 2π as go around the ring. This gives the soliton in vortex-like nature. The color variation might indicate the phase of the wave. In Fig. (3b), the concentric circle indicates that the density is highest at the centre and decreases as we move outwards. The color intensity represents the density level. The brightest colors signify the highest density, while the dark areas represent the lower density. The plot is smooth indicating a continuous distribution rather than discrete data points. Fig. (3c), shows the symmetric about the y-axis, indicating that the function is even. It has three turning points: two local maxima and one local minimum. The graph does not intersect the x-axis, indicating that the function has no real roots.

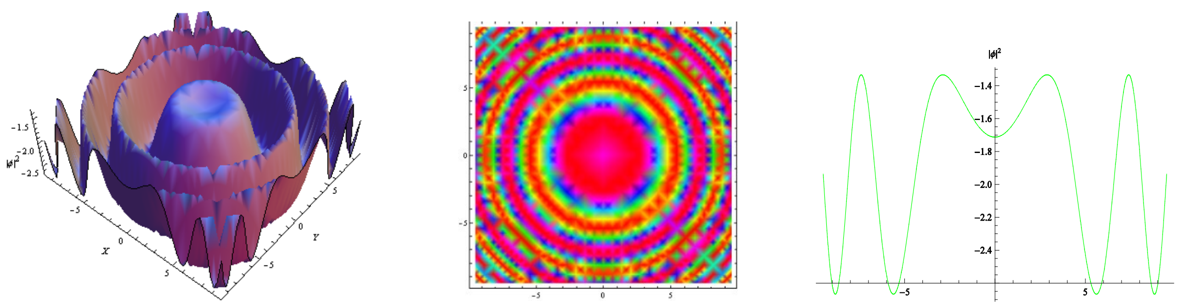

(b) (c)

Figure 4: Bright soliton collision in proteins

From Fig. (4a) exhibits a localized humb-like structure, which is a characteristic feature of these waves. It can travel over long distances without changing their shape. In Fig. (4b), different color represents different values of the function. The color scale can be customized, but generally, warmer colors indicate higher values, while cooler colors represent lower values. The brightness or saturation of the color also conveys information about the function values. The circular pattern in the plot suggests that the function values depend on the distance from the centre, indicating the radial symmetry. Fig. (4c), the figure represents a periodic function, the midline of the graph is shifted down from the x-axis. The amplitude of the soliton is approximately 0.8 units as the height of the wave from its midline.

4.4. Bright Soliton:

Solitons of this kind are known as bright solitons. They are wave fronts that have self-supported coherence in the nonlinear medium; typical of such a wave is the highest value of the amplitude at the centre of the wave front, with the amplitude decreasing to zero as the distance from the centre increases. This type of the soliton is possible owing to the delicate interplay between the nonlinearity which centres the wave and dispersion/diffraction that tends to diffuse it out [32]. Bright solitons are peaked in the space and the time in which they exist with the greatest intensity occurring at the centre of them. The envelope of the wave has a characteristic "hump." They are observed in media with self-focusing nonlinearity, which compensates for the dispersive effect of the medium [33][34].

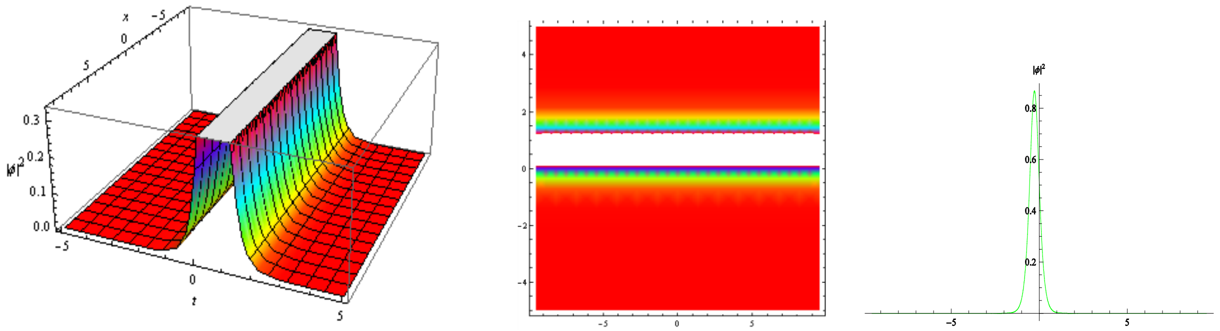

(b) (c)

Figure 5: Bright soliton collision in proteins

Fig. (5a), the wave is concentrated in a particular zone which however decreases very fast when distanced from the centre. It retains its profile and speed for long periods or distances even after coming into contact with other such waves. The wave can only exist in a medium with active nonlinear characteristics. The soliton has a distinct upturned bell shape suggesting that it is confined within certain limits. The soliton is translated in the direction of the x-axis without distortion in its form or velocity as depicted by the constant rise of the wave crest in the y- axis. Fig. (5b), it appears that the density map corresponds to the time-space variation of a quantity. The entire range is subdivided into two major regions, possibly indicative of two different conditions or systems. The yellow bright and green segments display regions which are of high density or intensity. The areas outlined in red are those of low density or intensity. There are wave-like formations present in the top half of the graph indicating oscillation or spread of some sort. Fig. (5c), takes the form of appears to be a bell shape, which is a feature of normal distribution or Gaussian function. The apex of the curve occurs when x = 0, which means that this is also the point at which the maximum of the function occurs. There is symmetry in the curve about the y-axis which implies that the function takes equal values for positive and negative x of the same magnitude. The curve dwindle rather quickly when x is not equal to 0 which means that the said function tends to zero as x tends positive or negative infinity.

4.5. Bright Soliton:

A dark soliton is a localized wave solution in a nonlinear system that appears as a localized dip (notch) or void in an otherwise continuous wave background. Unlike bright solitons, which are peaks of intensity, dark solitons are characterized by their phase shifts and intensity drops in systems with defocusing nonlinearity [35][36]. With regard to the dimension, the instability of the dark solitons is lower than that of bright solitons. They are known to be stable against small disturbances in many physical systems. Interaction of two dark solitons occurs in an elastic manner, i.e., the Das shape and the properties are not changed or destroyed. The velocity of the soliton is relative to the speed of the background fluid.

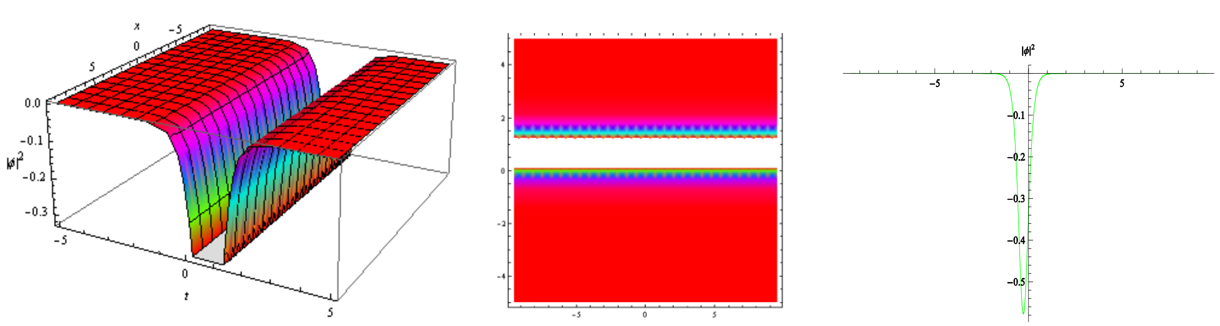

(b) (c)

Figure 6: Dark soliton interaction

Fig (6a), X axis is space, T is time, and the vertical axis is the height or amplitude of the wave.

The most important distinction of a soliton is its stable, unified profile that exists in a localized portion of the propagating medium. In this figure, the soliton looks like a pulse moving along the x-axis but does not change shape. Solitons are formed in circumstances where nonlinearity (where the speed of a wave is affected by its amplitude) balances out dispersion (where the wave becomes distorted in the space). That is why the soliton keeps its form. Fig (6b), the different colors used correspond to various intensities of the field plotted. For example, red shows higher values compared to blue which represents lower values. The soft edges between colors are indicative of a field which does not have sharp variations but changes smoothly over the area. The presence of recurring crests and troughs reveals that the field under consideration is periodic or oscillating. The color of the plot changes abruptly at the edges indicating boundaries or effects from the ambient medium. Fig (6c), the graph comes close to the y-axis (x = 0) but never actually the y-axis thus it has a vertical asymptote. This occurs when the rational function at that x value gives a zero in the denominator. As x approaches 0 from the left (x < 0), the graph decreases to -infinity. As x approaches O from the right (x > 0), the graph increases to +infinity. The graph seems to tend towards the x-axis (y=0) whenever x approaches positive or negative infinity indicating the presence of a horizontal axis at y=0. This is because usually the degree of the denominator is greater than the degree of the numerator, in the rational function.

4.6. Smooth Soliton:

A soliton of the class smooth describes some well-defined smooth or soft surfaces as those undergo no distortion or discontinuity. Solitons are self-sustaining wave forms that carry an envelope, and take a share of equal speed and distinct shape being pertained in several non-linear systems. Smooth solitons also behave as if they vanish or decay at infinity, that is the solution is 'in') placed in some finite region of space (or in time) [37]. Unlike those with sharp (i.e., shocks) discontinuities, smooth solitons do not exhibit any singularities or jumps. Soliton exhibit elastic collisions as they can collide with other solitons without changing their shape or speed. The soliton and its derivatives (up to some order) are defined and finite everywhere.

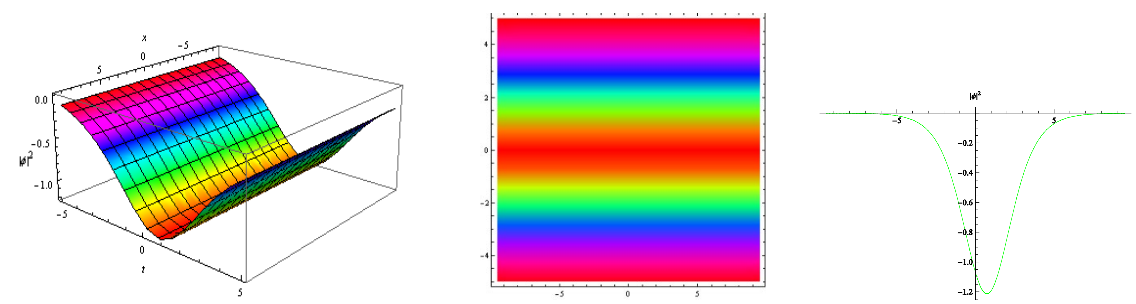

(b) (c)

Figure 7: Smooth soliton collision

Fig. (7a) seems to show that a single soliton solution of a nonlinear partial differential equation. The graph illustrates how the amplitude of the soliton changes over both space and time. The general structure of such a wave is the so-called localized wave, a pulse that is depicted in the figure above. Fig. (7b) displays the surface created by the density plot in two variable function space. A member of the variables is displayed along the x-axis and the other variable along the y-axis. The color encodes that the density of the data points are equally colored warmer color indicating more data points are present and cooler color indicating less data observed. Fig. (7c), the graph features a symmetrical shape that has a portion that extends downwards underneath the x-axis. The outline of the curve is like a concave up parabola with a "deeper dipping" section at the y-axis. The curve looks asymmetrical around the x-axis such that the left part is not equal to the right part. The lowest region on the graph, the least figure, seems to come around y = -1.2.

4.7. Parabolic Soliton:

Parabolic soliton is one of the spatial solitary wave structures of the soliton solutions to the nonlinear partial differential equation. As such, it implies that such a soliton has a temporal or spatial profile which mimics like parabola. These types of solitons can be found in numerous and varied physical and mathematical situations, most of the time in connection with equations of parabolic type or nature. The profile of the soliton is of parabolic type, or at some coordinate system, it acts like a parabola [38][39]. Occurs in system in which nonlinearity counteracts dispersion or diffusion. Propagates and maintain its compact structure in the same way as other solitons. Depending on the equation describing them, they may be stable during propagation as well as in interactions with other waves.

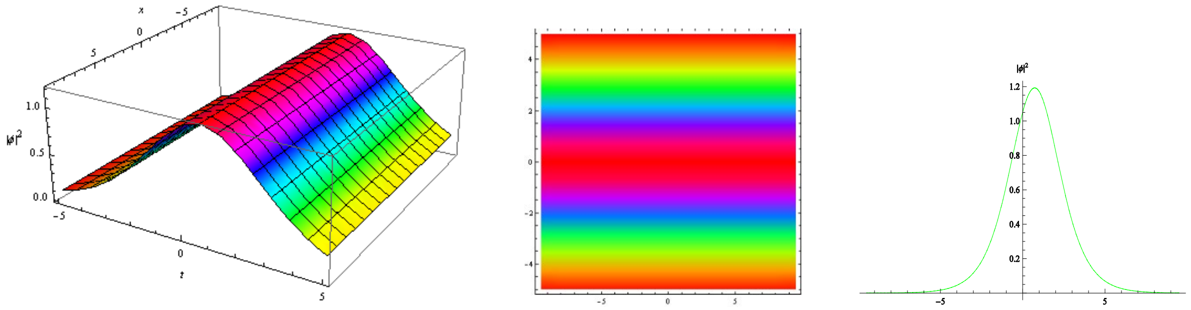

(b) (c)

Figure 8: Parabolic soliton interaction in proteins

Fig. (8a) illustrates the notion of a soliton, a solitary wave whose shape is preserved even as it moves with a certain velocity. The soliton body is depicted to have a hyperbolic secant like shape that is a typical shape for solitons in physical systems. It preserves its form when moving in the x-direction approximately over the time t. The amplitude height and the width of the soliton are fixed indicating its equilibrium state. The soliton is a localized wave form meaning that it exists with its energy in a bounded region. Fig. (8b), the color used in the plot corresponds to the range of a variable or a function. Usually, high values are depicted in warm colors (for instance, red, yellow) whereas lower values are drawn in cool colors (for example, blue). The color at any one point is a measure of the density or concentration of that variable at that point. Fig. (8c) is the bilaterally symmetrical forming at rounded peak at the mean. The point where the distribution is peak as depicted on the illustration represents the mean value on the data collected. Standard deviation indicates that how far the data on an average lies about the mean value. If you see the curves wider, it shows the standard deviation is larger than the narrow curves, which means that the standard deviation is smaller.

5. CONCLUSION

The present work addresses the effect of the inhomogeneity in a three-dimensional system of alpha-helices. A Hamiltonian model is proposed and perturbation theory is used to analyze the effects of inhomogeneity on the soliton propagation. A (3+1)-dimensional equation similar to the nonlinear Schrödinger (NLS) equation is constructed from the motion of equations describing the evolution of the system. This model validates solitons as an effective mechanism for the energy transfer in the alpha-helical proteins. Through the analysis, the total energy of the soliton solutions remains constant once the solitons collide because of the interplay of two modes of couplings: exciton-phonon and phonon-exciton. It is also utilized within the framework of perturbation techniques to formulate the numerous soliton solutions of the system referred to as the sine-cosine method. Eight distinct types of soliton propagation phenomena are studied in detail and the results are illustrated numerically, which shows the rich variety of soliton propagation with respect to inhomogeneity. The results are provided for the density profiles as well as for the time series describing the soliton collisions, which make it possible to understand the impact of inhomogeneity on the soliton propagation in the internal protein structure.

CONFLICT OF INTERESTS

None.

ACKNOWLEDGMENTS

None.

REFERENCES

Zitnik, M., Nguyen, F., Wang, B., Leskovec, J., Goldenberg, A., & Hoffman, M. M. (2018). Machine learning for integrating data in biology and medicine: Principles, practice, and opportunities. Information Fusion, 50, 71–91. https://doi.org/10.1016/j.inffus.2018.09.012

Salem, M. S. Z. (2018). Biological Networks: An Introductory Review. Journal of Proteomics and Genomics Research, 2(1), 41–111. https://doi.org/10.14302/issn.2326-0793.jpgr-18-2312

Fowler, S., Roush, R., & Wise, J. (2023d). Concepts of biology.

Molecular biology of the cell. (2002d).

Prevention of intravascular catheter-related infections. (2021). Indian Journal of Continuing Nursing Education, 22(1), 104. https://doi.org/10.4103/2230-7354.320831

Poulsen, N., & Kröger, N. (2004). Silica Morphogenesis by Alternative Processing of Silaffins in the Diatom Thalassiosira pseudonana. Journal of Biological Chemistry, 279(41), 42993–42999. https://doi.org/10.1074/jbc.m407734200

Bhutani, S. P. (2019). Chemistry of Biomolecules, Second Edition. CRC Press.

Prins, L. J., Reinhoudt, D. N., & Timmerman, P. (2001). Noncovalent synthesis using hydrogen bonding. Angewandte Chemie International Edition, 40(13), 2382–2426. https://doi.org/10.1002/1521-3773(20010702)40:13

Fox, A. J. S., Bedi, A., & Rodeo, S. A. (2009). The basic science of articular cartilage: structure, composition, and function. Sports Health a Multidisciplinary Approach, 1(6), 461–468. https://doi.org/10.1177/1941738109350438

Bittencourt, J. (2015). The power of carbohydrates, proteins, and lipids: How to Make Wise Choices in Diet and Nutrition. CreateSpace.

Bhat, S. (2012). Biomaterials. Springer Science & Business Media.

Adamatzky, A. (2002). Collision-Based computing. Springer Science & Business Media.

Debnath, L. (1994). Nonlinear water waves. Academic Press.

Cline, D. (2018). Variational principles in Classical mechanics: 2nd Edition.

Barone, M., & Selleri, F. (2012). Frontiers of Fundamental Physics. Springer Science & Business Media.

Yalçiner, A. C., Pelinovsky, E. N., Okal, E., & Synolakis, C. E. (2003). Submarine landslides and tsunamis. Springer Science & Business Media.

Fogel, M. B., Trullinger, S. E., Bishop, A. R., & Krumhansl, J. A. (1977). Dynamics of sine-Gordon solitons in the presence of perturbations. Physical Review. B, Solid State, 15(3), 1578–1592. https://doi.org/10.1103/physrevb.15.1578

Mandelstam, S. (1975). Soliton operators for the quantized sine-Gordon equation. Physical Review. D. Particles, Fields, Gravitation, and Cosmology/Physical Review. D. Particles and Fields, 11(10), 3026–3030. https://doi.org/10.1103/physrevd.11.3026

Cuevas-Maraver, J., Kevrekidis, P., & Williams, F. (2014). The sine-Gordon Model and its Applications: From Pendula and Josephson Junctions to Gravity and High-Energy Physics. Springer.

Davydov A S and Kisluka N I 1973 Phys. Stat. Sol. b 59 465.

Davydov A S and Kisluka N I 1976 Sov. Phys. JETP 44 571.

Davydov A S 1979 Phys. Scripta 20 387.

Davydov A S 1980 Sov. Phys. JETP 51 397.

A. S Davydov, J. Theor. Bio. 66 (1977) 376.

Haken, H. (2012). Synergetics: A Workshop Proceedings of the International Workshop on Synergetics at Schloss Elmau, Bavaria, May 2–7, 1977. Springer Science & Business Media.

Evans, C. R., Finn, L. S., & Hobill, D. W. (1989). Frontiers in numerical relativity. Cambridge University Press.

Huang, K. (2008). Quantum Field Theory: From Operators to Path Integrals. John Wiley & Sons.

Waldrop, M. M. (2019d). Complexity: The Emerging Science at the Edge of Order and Chaos. Open Road Media.

Butcher, P. N., & Cotter, D. (1990). The elements of nonlinear optics. Cambridge University Press

Landa, P. (2013c). Nonlinear oscillations and waves in dynamical systems. Springer Science & Business Media.

Chen, F. F. (2013c). Introduction to plasma physics and controlled fusion: Volume 1: Plasma Physics. Springer Science & Business Media.

Chen, F. F. (2013b). Introduction to plasma physics and controlled fusion: Volume 1: Plasma Physics. Springer Science & Business Media.

Ibach, H. (2006). Physics of surfaces and interfaces. Springer Science & Business Media.

Trillo, S. (2001). Spatial solitons. Springer Science & Business Media.

Shadrivov, I. V., Lapine, M., & Kivshar, Y. S. (2014). Nonlinear, tunable and active metamaterials. Springer.

Grant, I. P. (2007). Relativistic quantum theory of atoms and molecules: Theory and Computation. Springer Science & Business Media.

Zangwill, A. (1988). Physics at surfaces. Cambridge University Press.

Enns, R., & McGuire, G. (2013c). Nonlinear Physics with Maple for Scientists and Engineers. Springer Science & Business Media.

Trefethen, L. N. (2000). Spectral methods in MATLAB. SIAM.